Journal of Groundwater Science and Engineering
ISSN 2305-7068
Indexed by ESCI CABI CSA
Scopus GeoRef AJ CNKI

**Integration of geoelectric and hydrochemical approaches for delineation of groundwater potential zones in alluvial aquifer**

Qaisar Mehmood, Muhammad Arshad, Muhammad Rizwan, Shanawar Hamid, Waqas Mehmood, Muhammad Ansir Muneer, Muhammad Irfan, Lubna Anjum

Citation:
Qaisar Mehmood, Muhammad Arshad, Muhammad Rizwan, Shanawar Hamid, Waqas Mehmood, Muhammad Ansir Muneer, Muhammad Irfan, Lubna Anjum. Integration of geoelectric and hydrochemical approaches for delineation of groundwater potential zones in alluvial aquifer[J]. *Journal of Groundwater Science and Engineering*, 2020, 8(4): 366-380.

View online: https://doi.org/10.19637/j.cnki.2305-7068.2020.04.007

DOI: 10.19637/j.cnki.2305-7068.2020.04.007

# Integration of geoelectric and hydrochemical approaches for delineation of groundwater potential zones in alluvial aquifer

Qaisar Mehmood[1,2], Muhammad Arshad[1], Muhammad Rizwan[3,4*], Shanawar Hamid[5], Waqas Mehmood[2], Muhammad Ansir Muneer[1,6], Muhammad Irfan[7], Lubna Anjum[1]

[1] Department of Irrigation & Drainage, Faculty of Agricultural Engineering & Technology, University of Agriculture, Faisalabad, 38040, Pakistan.
[2] Department of Agriculture (Field Wing) Government of Punjab, Pakistan.
[3] Key Laboratory of Remote Sensing and Geospatial Science, Northwest Institute of Eco Environment and Resources, Chinese Academy of Sciences, Lanzhou 730000, China.
[4] University of Chinese Academy of Sciences, Beijing 100049, China.
[5] Khawaja Farid University of Engineering and Information Technology, Pakistan.
[6] Adaptive Research Farms, Agriculture Department (Extension & Research Wing) Punjab, Pakistan.
[7] PMU, Agriculture Department, Government of Punjab, Pakistan.

**Abstract: Geoelectric and hydrochemical approaches are employed to delineate the groundwater potential zones in District Okara, a part of Bari Doab, Punjab, Pakistan. Sixty-seven VES surveys are conducted with the Electrical Resistivity Meter. The resultant resistivity verses depth model for each site is estimated using computer-based software IX1D. Aquifer thickness maps and interpreted resistivity maps were generated from interpreted VES results. Dar-Zarrouk parameters, transverse resistance (TR), longitudinal conductance (SL) and anisotropy (λ) were also calculated from resistivity data to delineate the potential zones of aquifer. 70% of SL value is ≤3S, 30% of SL value is >3S. According to SL and TR values, the whole area is divided into three potential zones, high, medium and low potential zones. The spatial distribution maps show that north, south and central parts of study area are marked as good potential aquifer zones. Longitudinal conductance values are further utilized to determine aquifer protective capacity of area. The whole area is characterized by moderate to good and up to some extent very good aquifer protective area on the basis of SL values. The groundwater samples from sixty-seven installed tube wells are collected for hydro-chemical analysis. The electrical conductivity values are determined. Correlation is then developed between the EC (μS/cm) of groundwater samples vs. interpreted aquifer resistivity showing R2 value 0.90.**

**Keywords: Aquifer; Groundwater potential zone; Longitudinal conductance; VES**

**Received: 13 Jul 2020/ Accepted: 21 Sep 2020**

## Introduction

In Pakistan, agriculture is the second largest growing sector which is contributing 19.5% to GDP and 42% of employment of total labor force of the country (GOP, 2017). The population of the country is growing rapidly and reported 180 million and in 2025, it will be raised to 246 million as reported by (Aamer and Sabir, 2014). To meet the food requirements of this growing population, an increase in crop production is required which ultimately demands more water to grow these crops. Pakistan has three main sources of water (1) surface water, (2) rainfall and (3) groundwater. The country has the largest gravity flow canal irrigation system with capacity of 82 MAF water which unfortunately, supplies only half of its capacity due to obsolete system and improper management (Shakir *et al.* 2016). As arid to semi-arid conditions prevail in the country, considerable variation in

*Corresponding author. E-mail: rizwan514@lzb.ac.cn

amount and intensity of precipitation has been recorded which ranges from less than 10 mm in some parts of the country to more than 500 mm in other parts of the country (Abbas *et al.* 2014). The provision of adequate supply of fresh water due to rapid increase in population and industrialization has become a serious issue of the society. Water scarcity is escalating rapidly which causes severe drought conditions regularly and poses threats to agriculture economy of the country (Imran *et al.* 2018). The main reasons of water scarcity in the country are (1) poor surface water management, (2) urbanization, (3) rapid population growth, (4) silting of dams and reservoirs, (5) theft of irrigation water, (6) climate change and (7) lack of consensus between the provinces on construction of new reservoirs (Punthakey *et al.* 2016).

The irrigation water requirements for these situations have encouraged the farmers to explore groundwater to fulfill their needs (Alam and Olsthoorn, 2014). Groundwater exploration and abstraction has become more important, not only in Pakistan but all over the world. Due to high demand of irrigation water, farmers are mostly relying on the groundwater due to problems in surface water supplying. Furthermore, the farmers have no idea about location and depth of good quality groundwater layers and continuously install the irrigation tube wells in saline areas without proper investigation and exploring saline water which causes soil salinity problems (Sikandar e*t al.* 2017; Mehmood *et al.* 2020). The continuous pumping and overexploitation also result in the depletion of groundwater table in most parts of the country and the groundwater is inaccessible to poor farmers as pumping cost increases (Watto and Mugera, 2016). Various environmental factors, such as lithology, overburden thickness, climate change and drainage pattern *etc*. are responsible for the occurrence, distribution and flow of groundwater. Consequently, the groundwater is not uniformly distributed in terms of quality and quantity (Akinwumiju, 2016). Groundwater resource management has become more important due to the climate change, population increase and changing patterns of groundwater availability on spatial and temporal scale (Elliott *et al*. 2014). The continuous pumping of groundwater also causes the intrusion of saline water to fresh groundwater which is a serious threat to the irrigated agriculture in Pakistan (Basharat *et al*. 2015). Agricultural productivity can be increased by proper management of groundwater modeling (Shakoor, 2015).

In such conditions, a scientific and systematic approach which is easily available to farmers to overcome these problems has to be adopted. Several conventional approaches have been adopted by the researchers to delineate the groundwater potential zones. In this study, the Geoelectrical method with combination of Geographical Information System (GIS) technique and hydrochemical approach are employed to identify the groundwater potential zones. Geographical Information System is a very effective tool which had been used for studying groundwater and other natural resources in terms of its site suitability, mapping of its potential zones, assessment of aquifer vulnerability, groundwater modeling, solute transportation and spatial temporal mapping of groundwater table depth (Nas and Berktay, 2010; Charoenpong *et al.* 2012; Mohamaden *et al*. 2016). Geo-electrical method is cost-effectively and non-invasively to the farmers (Terry *et al.* 2017). Geo-electrical methods such as Vertical Electrical Sounding are commonly used for delineating and exploring the groundwater all over the world as well as for studying the subsurface lithology (Adagunodo *et al.* 2018; Manu *et al.* 2019). VES provides the knowledge of subsurface resistivity distribution which is based on the response of subsurface lithology when electric current is passed through the earth by some means. The subsurface resistivity information can be obtained by making arrangements on ground surface (El-Kadi, 2017). Geo-electrical techniques are often used for the investigation and assessment of groundwater quality in a specific area. Electrical resistivity technique has been proved a useful and reliable tool to locate the aquifer and to determine the potential of an aquifer (Adeniji *et al*. 2013). The use of Vertical Electrical Sounding survey has increased because of the advancement in numerical modeling solutions (Dor *et al.* 2011). Vertical Electrical Sounding technique is useful to study groundwater conditions and to evaluate the subsurface layers and the lithological conditions of the aquifer and this approach is also practicably applicable to correlate the lithological data of wells (Obianwu *et al.* 2015; Nwachukwu *et al.* 2019). Geophysical investigation is a quick and

easy approach for groundwater delineation rather than conventional method of test bore (Daraz *et al.* 2013).

GIS is a powerful tool which can integrate, analyze and manipulate large volume of spatial and non-spatial data. It is a big contribution to the groundwater exploration (Akinwumiju, 2016).

Keeping in view the groundwater related problems, this study is designed for the farmers of district Okara who heavily depend on the groundwater along with canal water to fulfill the crop water requirements. In this study, a combination of Geo-electric technique (VES) and GIS were used for the delineation of groundwater potential zone. The VES data had been utilized to develop spatial distribution maps, like iso-resistivity maps, layer thickness maps, longitudinal conductance and transverse resistance maps by employing GIS technology which are helpful for the identification of groundwater potential zones and to fix exact location of tube wells.

## 1 Study area

### 1.1 Geographical extent and climate

The research work was carried out in District Okara Punjab, Pakistan which is situated in Bari Doab (the area between rivers, Ravi and Satluj and Doab is local word). The geographical extent of District Okara is between 30.814 °N to 31.131 °N and 73.273 °E to74.211 °E with a total area of 4 377 km, bounded by districts Sheikhupura, Faisalabad and Sahiwal on west, district Kasur on north while districts Pakpattan and Bahawalnagar south and India on the east, see Fig. 1. The average temperature of Okara is 24.5°C. May and June are hottest months with maximum temperature 44°C and January is the coldest month with minimum temperature 2°C. The mean annual rainfall is 190 mm to 200 mm (Mehmood *et al*. 2020). The climate of the study area is semi-arid which depends on the irrigation water (Mujtaba *et al.* 2007).

### 1.2 Irrigation sources and cropping patterns

Total irrigated area of Okara is 616 000 hectares. About 12% of the area is irrigated by surface water supplies (canal irrigation system) while 78% of the area is irrigated by tube wells. The remaining area is irrigated by other source of irrigation (Bureau of Statistics, 2014). Okara has very fertile land with variety of cropping systems like rice wheat, maize-maize, and maize-wheat. Surface water is supplied through Lower Bari Doab Canal (LBDC) system which passes through the area and is the second largest irrigation system of Punjab with command area of 0.8 million hectares. The cropping intensity has been increased from 67% to 160% in the study area. The sustainability of agriculture is directly related to surface water supplies as wells as with the groundwater abstraction. Some part of culturable command area is water logged due to which the soils are saline. However, the fresh groundwater reservoirs are lying beneath most part of CCA (Basharat and Tariq, 2014; Shakir *et al.* 2016). The uncontrolled and unplanned abstraction of fresh groundwater to meet crop water requirements has remarkably depleted the water table in the area. According to Basharat (2013), a depletion rate of 0.55 m has been recorded during the last decade. The recharge in the area is mostly through leakage form irrigation canal networks and by percolation of rainwater. Although eastern rivers, Ravi and Satluj are passing from the area, touching its north-west and south-east boundaries these rivers have negligible impact on groundwater replenishment because the water flows in these rivers only in monsoon season. Therefore, the alluvium is saturated with fresh groundwater in upper layers a few meters deep. Resultantly, the soil salinity increases with depth. Mostly, the recharge in the area is at shallow depths and is less than 50 years old (Khan *et al.* 2016).

### 1.3 Geology and hydrogeology settings

The surficial geology of area is composed of soils of alluvial type with medium coarse and moderately textured, containing fine to very fine sand and silt and clay particles. The alluviums are brought from the Himalayan mountainous ranges by Indus River and its tributaries which are deposited on the semi-consolidated tertiary rocks (WAPDA, 1980). Sand pits have also been observed in most parts of the area at several meters depth. Several bore holes were drilled in the study area by Government agencies and organizations,

for groundwater exploration up to the depth of 300~400 m bottomed in the alluvial aquifers. Hence, there is no information revealed from these explanatory drilling bore holes about the presence of hard rocks as well no data available about the total thickness and depth of alluvial aquifer. The subsurface lithology from these drilling holes revealed that alluvial deposits comprise of predominant fine sandy particles along with silt, gravel and clay particles. The alluvium is relatively permeable and can store and transmit water (Alam and Olsthoorn, 2014; Hasan *et al*. 2017).

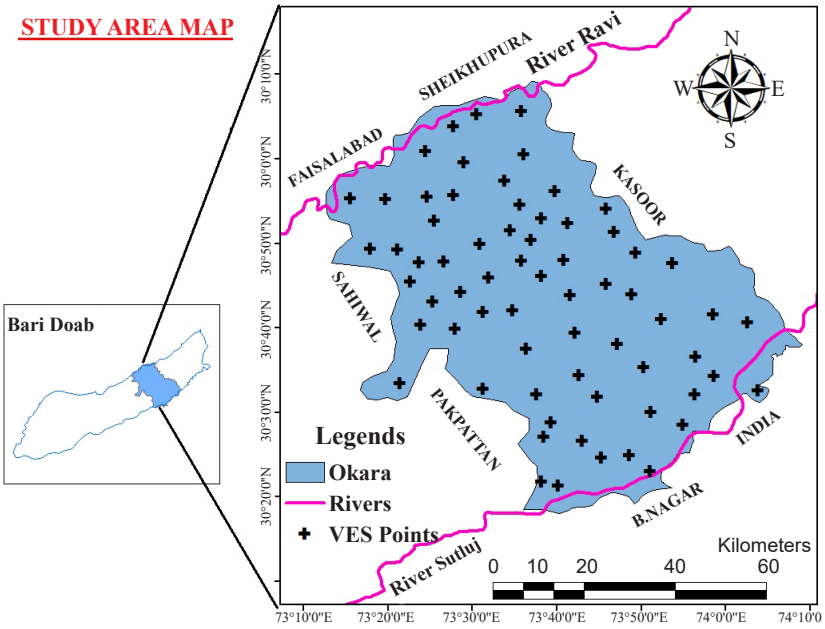


**Fig. 1** Study area map and location of VES points

## 2 Materials and methods

### 2.1 Geo-electrical technique (vertical electrical sounding survey)

Geo-electrical technique involves the inserting of electric current into the subsurface through electrodes and resulted potential difference is measured across potential electrodes placed on the ground at certain distance from current electrodes. The easiness or difficulty with which an electric current can pass through a material is the unit electrical resistivity of that material (Kearey *et al.* 2013). For this investigation, geo-electrical data is acquired by adopting Vertical Electrical Sounding technique. Electrical Resistivity Meter (ABEM Terrameter SAS-4000, Sweden) was used to conduct the VES surveys.

Sixty seven VES surveys were conducted in the study area. The GPS coordinates of each site were recorded. Schlumberger electrodes configuration with half current electrodes spacing (AB/2), ranging from 2 m to 200 m is utilized to conduct these surveys while potential electrodes spacing ranging from 0.5 m to 20 m is used. These four electrodes are placed in a straight line symmetrically about the center point as shown in Fig. 2.

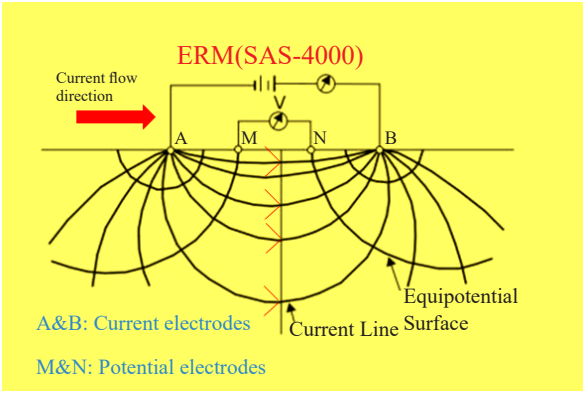


**Fig. 2** Hypothetical current and potential lines and position of current and potential electrodes (Schlumberger electrode configuration)

The field was energized by passing DC current

through current electrodes. This is because when AC current is passed through electrodes into the earth, the current density, due to skin effect phenomenon tends to concentrate towards the surface (Koefoed, 1979). To change the depth range under investigation the current electrodes are moved outward, keeping the potential electrodes fixed. However, when the ration between current to potential becomes too large the potential drops between the electrodes are too small, it is very difficult to measure with accuracy. In this situation, the potential electrodes are farther to each other. The constant selected current I (in milli amperes) and the potential difference V (in milli volts) is processed by the equipment and the resistance R is displaced for the corresponding reading. The mid-point of the electrodes is fixed as the VES location.

The apparent resistivity is calculated by the equation given below:

$$\rho_a = \pi \frac{\left(\frac{AB}{2}\right)^2 - \left(\frac{MN}{2}\right)^2 \times \frac{\Delta V}{I}}{MN} \quad (1)$$

$$\rho_a = K\left(\frac{\Delta V}{I}\right) \quad (2)$$

Where: $\rho_a$ is the resistivity of homogeneous earth. Since subsurface is heterogeneous in nature, the measured resistivity is the weighted average mean value of all the resistivities of the individual bodies which make the rock formation and commonly termed as "apparent resistivity" ($\rho_a$). The apparent resistivity depends upon the electric current *I*, potential difference *V* and geometric constant *K* (Kearey *et al.* 2013). *K* is Geometric constant which depends upon the electrodes arrangement and their configurations.

The geo-electric data obtained from these VES surveys were interpreted using IX1D (Interpex, 1-D) computer software. This software generated two kinds of resistivity models, smooth model and layered model, fitting the field data with least root mean square error (RMSE). The method of iteration is continuously applied until the fitting error between the field data and model curve approaches to minimum value and constant (Sikandar *et al*. 2017).

## 2.2 Calculating groundwater potential parameters

Resistivity ($\rho$) and thickness ($h$) of layers are two basic parameters which are obtained from geo-electric surveys. Maillet (1947) derived further geo-electrical parameters from these two parameters. These are longitudinal conductance (S), transverse resistance (T) and anisotropy ($\lambda$). These parameters are generally called Dar Zarrouk parameters.

For a single layer: Longitudinal conductance ($S_L$) = h/ρ

Transverse unit resistance ($T_R$) = h ρ

For n layers: $S_L = \sum \left(\frac{hi}{\rho i}\right) = \frac{h1}{\rho 1} + \frac{h2}{\rho 2} + \frac{h3}{\rho 3} \cdots \frac{hn}{\rho n}$ (3)

$$\left(\frac{hi}{\rho i}\right) = \frac{h1}{\rho 1} + \frac{h2}{\rho 2} + \frac{h3}{\rho 3} \cdots \frac{hn}{\rho n} \quad (4)$$

The value of longitudinal conductance depends upon the aquifer classification. The aquifer having poor longitudinal conductance are unprotected. The leachate and other hazardous liquid can infiltrate from dumping sites into the aquifer causing the groundwater contamination (Oladapo, 2007). The coefficient of anisotropy is >1 and <2. In some cases the value exceeds 2 depending upon the nature of aquifer and aquifer materials. The value of anisotropy exceeds 2 when the resistivity of the host material is higher as in case of dry sand and hard rocks (Singh, 2005). The coefficient of anisotropy is calculated by the relation given below:

$$\lambda = \sqrt{\left(\frac{\rho T}{\rho L}\right)} \quad (5)$$

Where: $\rho_L = H/S_L$ and $\rho_T = T_R/H$ are longitudinal resistivity and transverse resistivity respectively and H is total thickness of the aquifer.

# 3 Results and discussions

## 3.1 Interpretation of VES data

The VES surveys give the series of resistivity values with respect to current and potential electrodes spacing called apparent or iso-resistivity (Hasan *et al*. 2018). The apparent resistivity is the weighted average of all the true resistivity of materials in subsurface formation. The apparent resistivity values are modeled using software package and utilizing inverse iterative in order to delineate the thickness of the subsurface layers, types of geological curves and interpreted resistivity of respective layers. Three to four

geological layers with different resistivity values and with different curve types and layer thickness were demarcated in the study area depending upon the subsurface lithology of the area as given in Table 1 which shows that three and four geo-electric layers sections are detected. There are nine different geo-electric curve types, K type (18%), Q type (11%), H type (9%) and A type (4%) in the third layer section. Similarly, in the fourth layer section KQ (15%), KH (13%), HK (3%), AK (2%) and AQ (1%) have been obtained in the study area after interpreting the VES data. The shape of curve defines the characteristics of subsurface materials. The shape of curve is function of layer thickness, resistivity of the formation and number of the geo-electric layers (Michael *et al*. 2005).

**Table 1** Summary of interpreted results of 67 VES using IX1D software along with Dar-Zarrouk parameters ($T_R$= Transverse resistance, $S_L$ = Longitudinal conductance, λ = Coefficient of anisotropy)

| VES No. | Latitude | Longitude | Interpreted resistivity (Ω·m) | | | | Layer thickness (m) | | | Curve type | Groundwater parameters (DZ parameters) | | | Aquifer total thickness |
|---|---|---|---|---|---|---|---|---|---|---|---|---|---|---|
| | - | - | $\rho_1$ | $\rho_2$ | $\rho_3$ | $\rho_4$ | $h_1$ | $h_2$ | $h_3$ | - | $T_R(\Omega\cdot m^2)$ | Λ | $S_L$ Siemens | H(m) |
| 1 | 30.91039 | 73.59371 | 27 | 62 | 4 | 6 | 3 | 12 | 39 | KH | 981 | 1.02 | 10 | 54 |
| 2 | 30.79600 | 73.39500 | 19 | 58 | 2 | | 3 | 16 | | K | 985 | 1.83 | 0.43 | 19 |
| 3 | 30.67300 | 73.39800 | 23 | 51 | 7 | 2 | 3 | 17 | 57 | KQ | 1 335 | 1.05 | 8.61 | 77 |
| 4 | 30.87800 | 73.42500 | 39 | 71 | 10 | | 3.35 | 11 | | K | 912 | 1.39 | 0.24 | 14.35 |
| 5 | 30.71900 | 73.42200 | 29 | 41 | 14 | 82 | 4 | 17 | 75 | KH | 1 863 | 1.01 | 5.91 | 96 |
| 6 | 30.75737 | 73.37778 | 20 | 39 | 14 | | 3 | 19 | | K | 801 | 1.03 | 0.64 | 22 |
| 7 | 30.85860 | 73.57402 | 36 | 53 | 16 | 11 | 1.33 | 11.5 | 49 | KQ | 1 441 | 1.09 | 3.32 | 61.83 |
| 8 | 30.73818 | 73.47733 | 34 | 165 | 19 | 4 | 2 | 6.5 | 24 | KQ | 1 597 | 1.03 | 1.36 | 32.5 |
| 9 | 30.79799 | 73.44399 | 52 | 226 | 27 | 157 | 2 | 17 | 89 | QH | 6 349 | 1.12 | 3.41 | 108 |
| 10 | 30.55700 | 73.35600 | 54 | 45 | 116 | 17 | 2 | 7 | 26 | HK | 3 439 | 1.12 | 0.42 | 35 |
| 11 | 30.82042 | 73.35177 | 56 | 35 | 24 | | 1 | 12 | | K | 476 | 1.38 | 0.36 | 13 |
| 12 | 30.69832 | 73.52022 | 56 | 56 | 38 | 1 | 1 | 10 | 92 | KQ | 4 112 | 1.36 | 2.62 | 103 |
| 13 | 30.83214 | 73.51469 | 62 | 286 | 135 | 44 | 2 | 10.5 | 34 | KQ | 7 717 | 1.07 | 0.32 | 46.5 |
| 14 | 31.08800 | 73.50800 | 65 | 10 | 47 | | 8 | 14.7 | | H | 667 | 1.01 | 1.59 | 22.7 |
| 15 | 31.01600 | 73.40800 | 72 | 52 | 23 | 8 | 4 | 16.5 | 62 | KQ | 2 572 | 1.11 | 3.07 | 82.5 |
| 16 | 30.99367 | 73.48354 | 70 | 93 | 11 | | 5 | 59 | | K | 5 837 | 1.00 | 0.71 | 95 |
| 17 | 31.09400 | 73.59600 | 64 | 94 | 13 | | 7 | 53 | | K | 5 430 | 1.06 | 0.67 | 70 |
| 18 | 30.95701 | 73.56341 | 34 | 10 | 92 | | 6 | 48 | | H | 684 | 1.17 | 4.98 | 56 |
| 19 | 30.92900 | 73.46239 | 36 | 34 | 83 | | 8 | 63 | | A | 2 430 | 1.09 | 2.08 | 84 |
| 20 | 31.06400 | 73.46300 | 39 | 34 | 78 | 12 | 8 | 40 | 52 | KQ | 5 728 | 1.00 | 2.05 | 100 |
| 21 | 31.00927 | 73.60100 | 42 | 22 | 10 | | 5 | 56 | | Q | 1 442 | 1.01 | 2.66 | 88 |
| 22 | 30.92000 | 73.32900 | 61 | 37 | 99 | | 7 | 69 | | A | 2 980 | 1.08 | 1.98 | 96 |
| 23 | 30.92500 | 73.41000 | 72 | 83 | 30 | 9 | 6 | 52 | 42 | H | 6 008 | 1.00 | 2.11 | 128 |
| 24 | 30.92200 | 73.25900 | 70 | 10 | 38 | | 2 | 33 | 49 | KQ | 2 332 | 1.08 | 4.62 | 87 |
| 25 | 30.75381 | 73.76415 | 72 | 67 | 29 | 7 | 4 | 51 | 49 | HK | 5 126 | 1.01 | 2.51 | 108 |
| 26 | 30.82200 | 73.29800 | 70 | 82 | 52 | | 5 | 59 | 43 | K | 7 424 | 1.01 | 1.62 | 108 |
| 27 | 30.53100 | 73.74684 | 55 | 24 | 16 | | 6 | 20 | | Q | 810 | 1.12 | 9.94 | 26 |
| 28 | 30.41010 | 73.75495 | 13 | 79 | 13 | 19 | 3 | 8 | 157 | KH | 2 712 | 1.03 | 10.41 | 168 |
| 29 | 30.67700 | 74.04300 | 8 | 23 | 80 | | 5 | 57 | | K | 1 351 | 1.04 | 3.1 | 85 |
| 30 | 30.62500 | 73.60600 | 9 | 65 | 11 | | 9 | 76 | | K | 5 021 | 1.09 | 2.17 | 85 |

Table 1 (Continued)

| VES No. | Latitude | Longitude | Interpreted resistivity (Ω·m) | | | | Layer thickness (m) | | | Curve type | Groundwater parameters (DZ parameters) | | | Aquifer total thickness |
|---|---|---|---|---|---|---|---|---|---|---|---|---|---|---|
| | - | - | $\rho_1$ | $\rho_2$ | $\rho_3$ | $\rho_4$ | $h_1$ | $h_2$ | $h_3$ | - | $T_R$(Ω·m$^2$) | Λ | $S_L$ Siemens | H(m) |
| 31 | 30.66464 | 73.46537 | 12 | 89 | 13 | 19 | 3 | 11 | 33 | KH | 1 444 | 1.02 | 2.91 | 47 |
| 32 | 30.35500 | 73.67000 | 12 | 84 | 44 | 11 | 6 | 55 | 23 | HK | 5 704 | 1.06 | 1.68 | 84 |
| 33 | 30.45100 | 73.64100 | 47 | 9 | 6 | | 8 | 54 | | Q | 862 | 1.62 | 6.17 | 92 |
| 34 | 30.69400 | 73.97600 | 6 | 89 | 5 | 81 | 1 | 8.7 | 58 | KH | 1 070 | 1.09 | 9.86 | 67.7 |
| 35 | 30.44335 | 73.71715 | 14 | 81 | 24 | | 12 | 22 | | K | 1 950 | 1.03 | 1.13 | 34 |
| 36 | 30.38452 | 73.85146 | 30 | 81 | 8 | 25 | 3 | 12 | 109 | KH | 1 934 | 1.23 | 9.1 | 124 |
| 37 | 30.54589 | 73.52160 | 20 | 36 | 82 | 138 | 1 | 18 | 36 | AK | 3 620 | 1.32 | 0.99 | 55 |
| 38 | 30.47500 | 73.91500 | 59 | 49 | 15 | | 11 | 36 | | Q | 2 413 | 1.16 | 0.92 | 57 |
| 39 | 30.58921 | 73.83889 | 10 | 11 | 29 | | 1 | 10 | | A | 120 | 1.13 | 10.01 | 11 |
| 40 | 30.53500 | 73.62700 | 37 | 52 | 26 | 12 | 2 | 13 | 103 | KH | 3 428 | 1.58 | 4.27 | 118 |
| 41 | 30.60987 | 73.94022 | 41 | 19 | 30 | | 5.5 | 56 | | H | 1 290 | 1.38 | 9.9 | 66.5 |
| 42 | 30.79400 | 73.89500 | 47 | 64 | 27 | 82 | 1 | 23 | 78 | KQ | 4 171 | 1.32 | 1.01 | 102 |
| 43 | 30.48000 | 73.65500 | 47 | 32 | 29 | | 3 | 39 | | Q | 1 389 | 1.08 | 1.28 | 42 |
| 44 | 30.81416 | 73.82225 | 22 | 103 | 28 | 87 | 2 | 9 | 90 | KH | 3 491 | 1.00 | 3.39 | 101 |
| 45 | 30.73300 | 73.81500 | 22 | 127 | 5 | | 3 | 46 | | Q | 5 908 | 1.00 | 0.5 | 54 |
| 46 | 30.54270 | 74.06452 | 35 | 108 | 14 | | 2 | 48 | | Q | 5 254 | 1.04 | 0.5 | 60 |
| 47 | 30.68400 | 73.87300 | 17 | 35 | 78 | 13 | 2 | 10 | 37 | AK | 3 270 | 1.02 | 0.88 | 49 |
| 48 | 30.53541 | 73.93927 | 472 | 271 | 281 | | 3 | 24 | | H | 7 920 | 1.15 | 0.09 | 27 |
| 49 | 30.57300 | 73.71000 | 10 | 40 | 7 | | 2 | 35 | | K | 1 420 | 1.00 | 1.08 | 37 |
| 50 | 30.57183 | 73.97724 | 7 | 36 | 23 | | 5 | 28 | | K | 1 043 | 1.05 | 1.49 | 33 |
| 51 | 30.65709 | 73.70189 | 44 | 147 | 247 | 36 | 1 | 20 | 28 | AK | 9 900 | 1.10 | 0.27 | 49 |
| 52 | 30.73135 | 73.69253 | 45 | 16 | 7 | | 6 | 70 | | Q | 1 390 | 1.02 | 4.51 | 96 |
| 53 | 30.36300 | 73.63600 | 39 | 52 | 24 | | 6 | 42 | | K | 2 418 | 1.09 | 0.96 | 48 |
| 54 | 30.63550 | 73.78595 | 28 | 68 | 24 | | 5 | 21 | | K | 1 568 | 1.14 | 0.49 | 26 |
| 55 | 30.50100 | 73.85200 | 27 | 71 | 4 | | 14 | 59 | | K | 4 567 | 1.02 | 1.35 | 93 |
| 56 | 30.41499 | 73.80934 | 14 | 45 | 26 | 119 | 8 | 23 | 99 | KQ | 3 721 | 1.06 | 4.89 | 130 |
| 57 | 30.93588 | 73.66342 | 15 | 9 | 13 | | 4.5 | 68 | | H | 680 | 1.20 | 7.86 | 92.5 |
| 58 | 30.76601 | 73.53270 | 17 | 11 | 28 | | 4 | 62 | | H | 750 | 1.06 | 5.87 | 66 |
| 59 | 30.85560 | 73.77983 | 15 | 8 | 14 | | 7 | 38 | | H | 409 | 1.03 | 5.22 | 45 |
| 60 | 30.87400 | 73.68900 | 68 | 65 | 4 | | 6 | 39 | | Q | 2 943 | 1.00 | 0.69 | 48 |
| 61 | 30.79870 | 73.59703 | 53 | 90 | 5 | | 9 | 12 | | K | 1 557 | 1.06 | 0.30 | 21 |
| 62 | 30.76900 | 73.63600 | 40 | 106 | 8 | 10 | 1 | 10 | 37 | KH | 1 396 | 1.06 | 4.74 | 48 |
| 63 | 30.90210 | 73.76359 | 59 | 99 | 4 | | 5 | 28 | | A | 3 067 | 1.04 | 0.37 | 33 |
| 64 | 30.70100 | 73.58000 | 45 | 63 | 3 | | 3 | 31 | | K | 2 088 | 1.01 | 0.56 | 34 |
| 65 | 30.84065 | 73.61586 | 65 | 65 | 15 | | 2 | 29 | | Q | 2 015 | 1.01 | 0.48 | 31 |
| 66 | 30.80100 | 73.68000 | 5 | 3 | 7 | | 3 | 18 | | H | 569 | 1.03 | 6.6 | 21 |
| 67 | 30.88200 | 73.63600 | 48 | 34 | 22 | | 4 | 41 | | K | 1 586 | 1.00 | 1.29 | 45 |

'K' type curves are being prevalent among three the third layer curves. The resistivity relationship of such type of curves is presented as $\rho_1 < \rho_2 > \rho_3$, indicating three geo-electric layers. The relationship describes that the resistivity value in the middle of section is maximum and then gradually decreases with depth. It also reveals the presence of good quality water in middle or at shallow

depth. Similarly, in four geo-electric layers, the sounding curve, "KQ" type curve has been found at maximum sites. The resistivity relationship for such type of curves is presented as $\rho_1 < \rho_2 > \rho_3 > \rho_4$. Such type of curve indicates the presence of low resistivity layer at the bottom of aquifer which proves the availability of saline water in deeper formations.

## 3.2 Verification of VES results by test drilling

One site VES-42 was selected for drilling. In most part of the area the good quality water is available at shallow depth. The VES results show presence of good quality water in deeper layers at this site. Therefore, this site was selected for validation and verification of VES results with actual borehole data. As per VES survey, top layer at this site is composed of sandy soil material with resistivity of 47 Ω·m up to the depth of 1 m with conserved moisture contents which is followed by a second layer having resistivity of 64 Ω·m and thickness of 23 m. This layer is composed of coarse sand and silt with marginal to good quality water. The third layer starts from 24 m and extends to 78 m with resistivity of 27 Ω·m. This layer is composed of hard clay containing saline water quality. The fourth layer has infinite thickness and resistivity of 82 Ω·m composed of coarse sand and gravels. The groundwater quality in this zone is found good. The groundwater and lithology samples were collected during the drilling and were tested in laboratory. The lithological data has close agreement with the interpreted results of VES surveys as shown in Fig. 3. The EC value is 1 060 μS/cm between the thickness of 78 m to 140 m because the bore was drilled to the depth of 140 m. The EC value falls in safe limit of good quality water criterion as prescribed by WAPDA (1981).

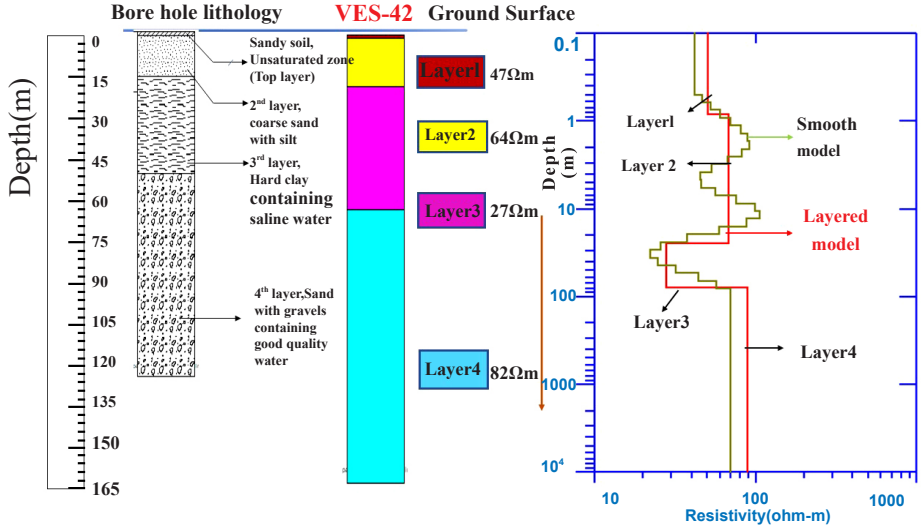


**Fig. 3** Verification of VES results by test drilling

## 3.3 Spatial distribution of interpreted resistivity of layers

Spatial distribution maps of interpreted resistivity of all the four geo-electric layers (Layer 1, Layer 2, Layer 3 and Layer 4) have been generated on the basis of VES results given in Table 1. These interpreted resistivities were plotted at depths above water table (Unsaturated zone), 30 m, 60 m and 150 m. Fig. 4 (a) shows the spatial distribution map of layer 1. The average resistivity of this layer is 43 Ω·m. This layer is composed of unsaturated material having sand and clay material and located above the water table. Fig. 4(b) shows spatial distribution map of layer 2. The average resistivity of second layer is 66 Ω·m. The average thickness of second layer is 30 m. This layers contains saturated zones at shallow depth below water table at different locations with unconfined aquifer. This thin layer is also part of the top layer due to varying soil moisture content and sand ratio at many sites as mentioned in interpreted results in Table 1. Also the variability in layer thickness at 45% VES points in terms of its depth, indicating the homogeneity in subsurface layered media. Although, 20% sites have resistivity more than

100 Ω·m in second layer section, indicating the saturated sand deposits containing good quality water but second layer does not have good potential for groundwater exploration for irrigation purposes due to shallow depth and deep water table ranging from 10 m to 14 m. Fig. 4(c) shows spatial distribution map of resistivity of layer 3. The resistivity value ranges from 2 Ω·m to 281 Ω·m. The average thickness of layer 3 is 60 m. The layer contains potential aquifer tapped by many high-yielding water wells in the study area. This layer is located below the water table depth in the soil strata containing saturated sand which is the best medium for groundwater presence, regardless of its quality which mainly depends upon the salts present in the water. The resistivity values give the idea of poor, marginal and good quality water availability in this layer. High interpreted resistivity values ranging from 98 Ω·m to 279 Ω·m are present in small patches in central, north and west parts of study area indicating the presence of course sand mixed with clay. Resistivity value ranging from 38 Ω·m to 98 Ω·m in S-E and N-W and in small patches in west direction confirms the availability of fine sand containing good quality water. The resistivity ranging from 2 Ω·m to 38 Ω·m composed of clay mixed with sand containing brackish to poor quality water. Fig. 4(d) shows the spatial distribution of resistivity of layer 4. The resistivity values are ranging from 1 Ω·m to 157 Ω·m. This layer has infinite thickness and extends to aquifer basement or depth of current penetration. The layer contains clay and clay sand containing saline/brackish quality of groundwater at shallow depth with resistivity ranging from 1 Ω·m to 20 Ω·m. Clay with sand containing poor to marginal quality water with resistivity values ranging from 20 Ω·m to 58 Ω·m appears in S-W, S-E and southern parts. Similarly, good quality water with fine sand particles in patches with resistivity values ranging from 58 Ω·m to 156 Ω·m is demarcated in east, south and west parts. The results also show that only layer 3 and layer 4 are situated in saturated zone and contain potential groundwater.

Groundwater samples from 67 tube wells are also collected at different depths. The samples were collected from the tube wells at the depth ranging from 80 to 200 feet which were located very close to the VES points. These groundwater samples were analyzed in laboratory to determine the (Electrical Conductivity) EC (μS/cm) of water to develop a correlation between the EC and interpreted resistivity/resistivity values of aquifer at the same depth. A correlation is developed between EC of groundwater and aquifer interpreted resistivity. Fig. 5 shows good quality groundwater can be explored with interpreted resistivity values between 50 Ω·m and 98 Ω·m (EC<1 500 μS/cm), marginal to good quality water can be explored with interpreted resistivity value from 22 Ω·m to 50 Ω·m (EC 1 500~2 700 μS/cm) and below 22 Ω·m interpreted resistivity value indicates saline brakish water (EC>2 700 μS/cm). The criterion of groundwater quality based on EC values is reported by WAPDA (1981).

### 3.4 Spatial distribution of layer thickness

The spatial distribution of geo-electric layer thickness for layer 1, layer 2 and layer 3 are presented in Fig. 6. The thickness of the fourth layer is infinite, so the map of layer 4 has not been generated. The thickness ranges from 1 m to 14 m, 7 m to 76 m and 23 m to 157 m for layer 1, layer 2 and layer 3 respectively. The increase in thickness from top surface to bottom of aquifer shows the homogeneity of the aquifer material and also indicates the aquifer potential to store water. Maximum thickness of layer 1, layer 2 and layer 3 is 6~14 m, 43~76 m and 138~156 m as shown in Fig. 6a, Fig. 6b and Fig. 6c respectively. The maximum thickness value in all the three layers has been noted in north and south parts of study area along the sides of Satluj and Ravi rivers accordingly. The higher thickness value in these side may be due to the formation of alluvial aquifer which is developed by the silt deposits brought by these rivers from the mountains.

### 3.5 Estimation of aquifer potential zones using DZ parameters

The aquifer characteristics and groundwater potential zones can be differentiated and estimated by Dar-Zarrouk parameters. Transverse resistance ($T_R$) and longitudinal conductance ($S_L$) are two basic Dar-Zarrouk parameters which are derived from resistivity and thickness of aquifer. The resistivity and thickness have been determined by the VES surveys. The area is divided into three

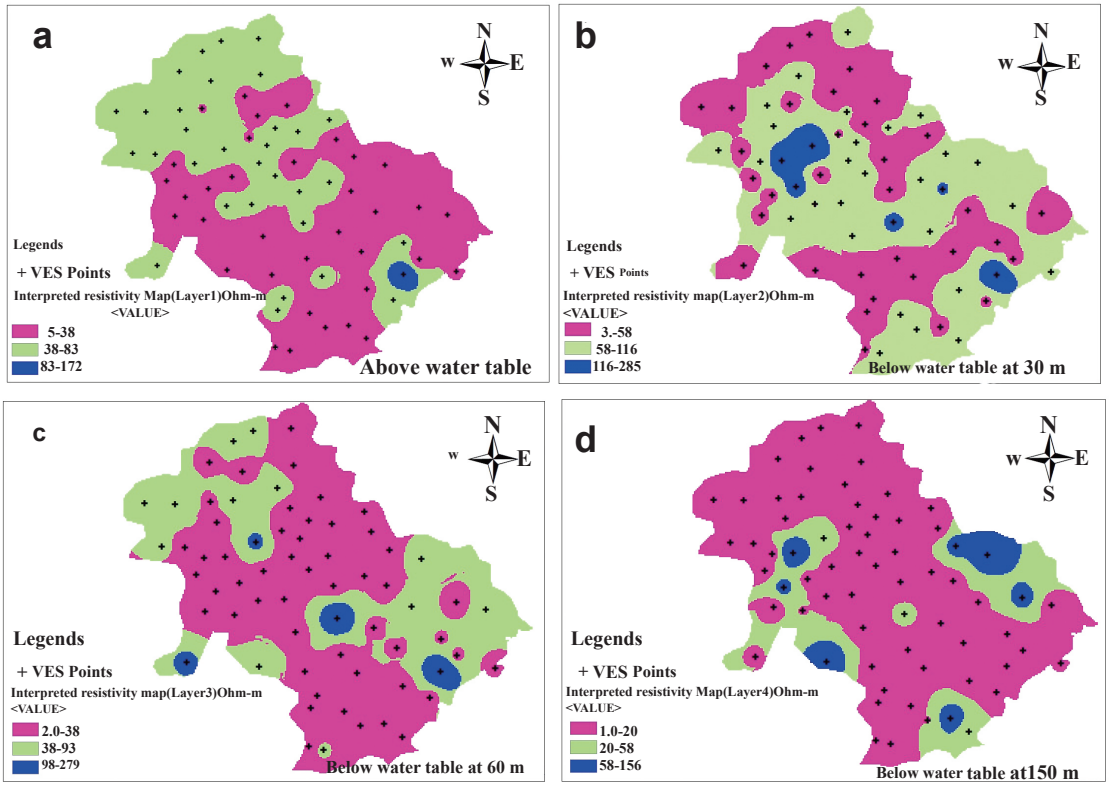


**Fig. 4** Spatial distribution map of interpreted resistivity of layers1, 2, 3, and 4 respectively

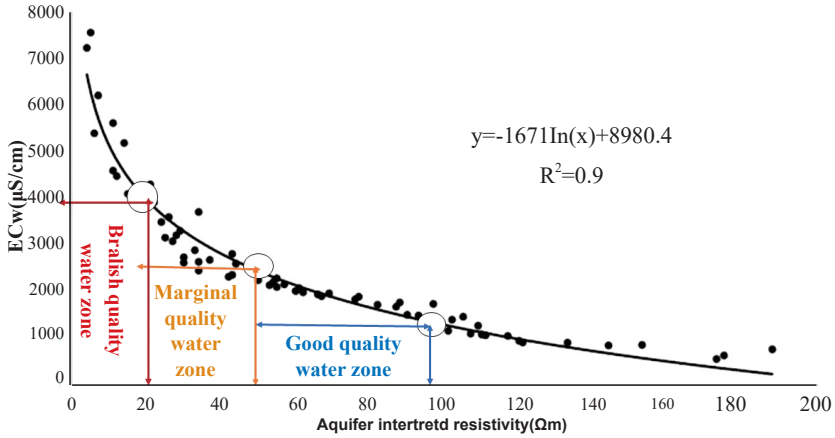


**Fig. 5** Relation between aquifer interpreted resistivity and groundwater EC of installed tube wells

potential zones as high, medium and low potential zones on the basis of longitudinal conductance and transverse resistance values. The spatial distribution of these parameters was generated as shown in Fig. 7(a, b). The numeric values of Dar-Zarrouk parameters were tabulated in Table 1.

Longitudinal conductance with low values indicating shallow basement whereas the high value showing deeper basement. In the present investigation, about 70% VES locations have SL values ≤3 (Siemens) indicating the shallow to medium deep basement while the remaining sites have SL values >3 (Siemens) showing deeper basements. The longitudinal conductance values ranging from 0.11S to 2.72S show high potential aquifer zone with availability of good quality water. The values range from 2.72S to 4.82S indicating medium potential zone with marginal quality water. Whereas, the values ranging from 4.82S to 10.38S represent low potential zone. Fig. 7(a) shows that north part, central part and few points in south parts of area are subjected to low SL representing potential aquifer zones with good quality of water.

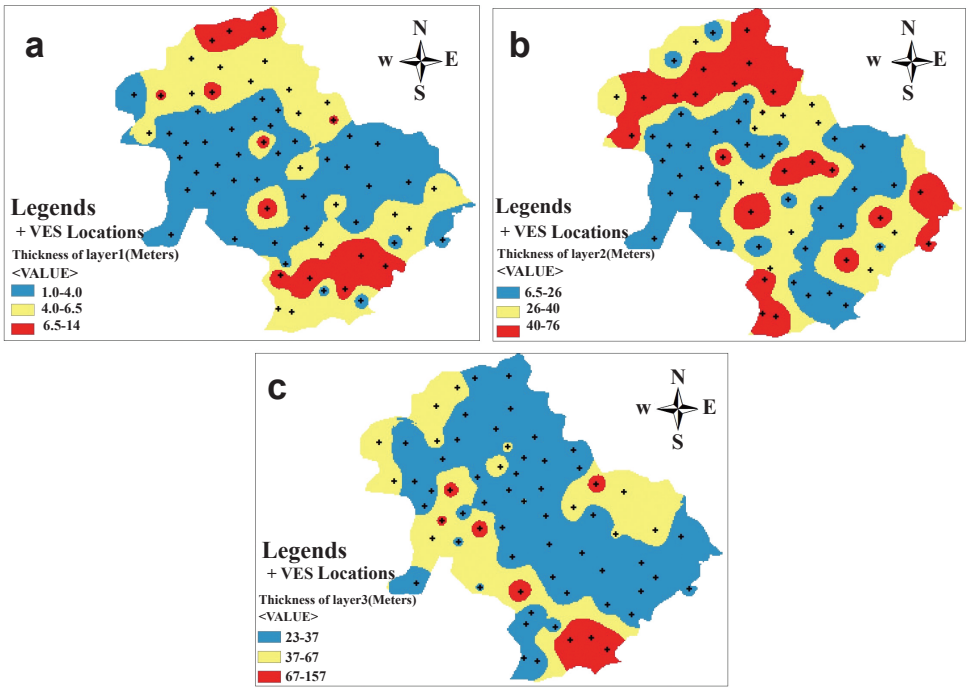


**Fig. 6** Spatial distribution maps of thickness of layer 1, layer 2, and layer 3

Furthermore, the longitudinal conductance values offer the aquifer protection capacity. Higher SL value indicates good aquifer protection capacity and vice versa. Oladapo and Akintorinwa (2007) classified the area into excellent, good, moderate, poor and week protective capacity zones on the basis of longitudinal conductance values. Longitudinal conductance values and corresponding aquifer protective capacity are shown in Table 2.

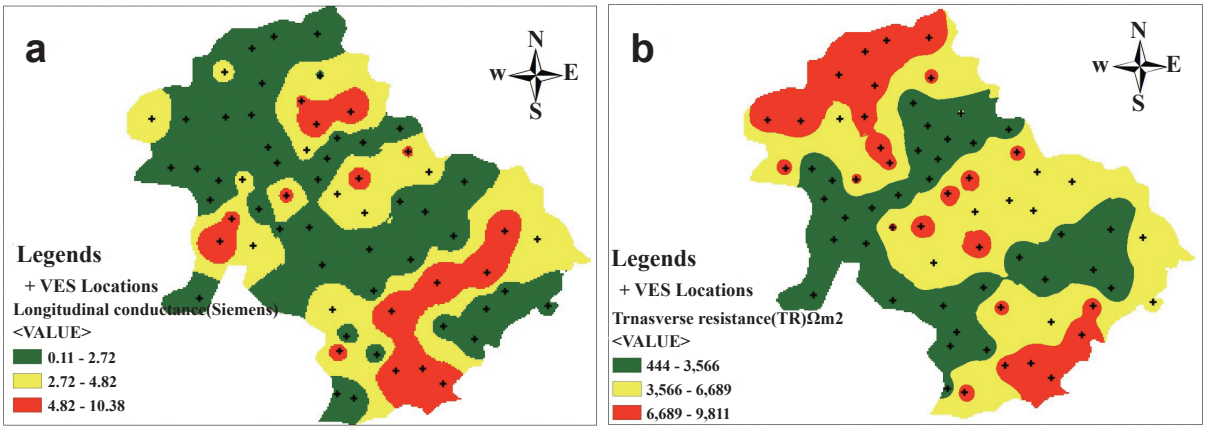


**Fig. 7** Spatial distribution map transverse resistance and longitudinal conductance

**Table 2** Classification of aquifer protective capacity w.r.t. to SL values as reported by (Oladapo and Akintorinwa, 2007)

| Sr. No. | Longitudinal conductance ($S_L$) (Siemens) | Aquifer protective capacity |
|---|---|---|
| 1 | >10 | Excellent |
| 2 | 5~10 | Very good |
| 3 | 0.7~4.9 | Good |
| 4 | 0.2~0.69 | Moderate |
| 5 | 0.1~0.19 | Weak |
| 6 | <0.1 | Poor |

Thus longitudinal conductance values given in Table 1 derived from the VES surveys data show only the points VES-1, VES-28 and VES-39 exhibit the $S_L$ >10S and fall in excellent aquifer protective capacity category which is only 4% of the area. Similarly, twelve points fall in category where $S_L$ values range from 5S to 10S which is 18% of the total area showing very good aquifer protective capacity area. Thirty five VES locations (52%) indicate good aquifer protective capacity as these points fall in the category where $S_L$ ranging from 0.7S to 4.9S. Sixteen VES locations specifying moderate aquifer protective capacity zone have the $S_L$ values ranging from 0.2S to 0.69S at these locations which is 24% of total area. Whereas, only one VES location (1%) envisages poor aquifer protective capacity as $S_L$< 0.1. Thus it has been suggested from the present study, the whole area is characterized by moderate to good and up to some extent very good aquifer protective area on the basis of $S_L$ values. Longitudinal conductance value increases, indicating an increase in clay content thus decrease in transmissivity of the aquifer which provides protection to underlying aquifer.

The transverse resistivity ($T_R$) values range from 120 Ω·m$^2$ at VES39 to 9 900 Ω·m$^2$ at VES-51 as given in Table 1. High transverse resistance values ranging from 6 689 Ω·m$^2$ to 9 811 Ω·m$^2$ can be seen in north, south and at some points in central parts of study area indicating good quality water zones. The values ranging from 3 566 Ω·m$^2$ to 6 889 Ω·m$^2$ represent medium potential zone with marginal quality of water. The marginal zones are scattered almost in every corner of the area. Similarly, the values ranging from 444 Ω·m$^2$ to 3 566 Ω·m$^2$ show low potential aquifer zone with saline and brackish water. Low potential zones are demarcated in SW, SE and eastern sides of area Fig. 7(b).

The coefficient of anisotropy (λ) is a function of transverse resistivity and longitudinal resistivity. The value of coefficient of anisotropy is ranging from 1 to 1.83 which is in the general range and not exceeding to 2. The values of anisotropy are given in Table 1 and the spatial distribution of values is shown in Fig. 8. The value of anisotropy indicates the hardness and compaction of layers and aquifer basement. If the value of anisotropy is greater than 2, it indicates the materials with higher resistivity other than rock formation. In present studies the values ranging from 1 to 1.83 predict the non-availability of rock formation in basement in study area. Therefore these areas are subjected to less porosity and permeability. The areas having λ >1 and the value not exceed to 1.5 are scrutinized as potential groundwater zones (Yeboah-Forson and Whitman, 2014).

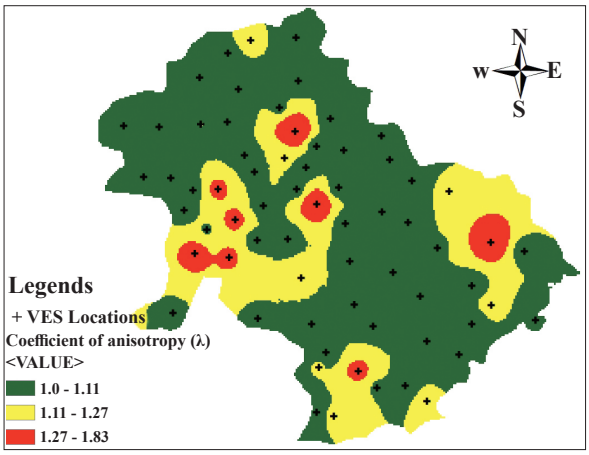


**Fig. 8** Spatial distribution map of coefficient of anisotropy

## 4 Conclusions

The investigations carried out in this study show that VES is useful technique to explore the groundwater quality in an aquifer. Dar-Zarrouk parameters were used in this study which are calculated from basic resistivity parameters, thickness and apparent resistivity and provide better solution to estimate the aquifer characteristics and groundwater potential zones of the aquifer.

The resistivity obtained from field investigation provides useful information about the subsurface lithology and characteristics of aquifer after interpreting the resistivity values using computer software. The results from 67 VES study points showed that 63% points have three layers while 37% of the point have four geo-electric layers. A high interpreted resistivity value (472 ohm-m) has been observed at VES-48 in top layer which is the indication of presence of dry sand patches. The spatial distribution maps of longitudinal conductance and transverse resistance indicate that north, south and patches in central parts of study area have high potential zones with good quality water. It has also been estimated from the

spatial distribution of interpreted resistivity that the good quality water is available at shallow depths in north and central parts of the area while good quality water is available in deeper layers in south parts of the area. The results also show that 4% of the study area fall in excellent, 18% very good, 52% good 24% moderate aquifer protective capacity while only 1% of the study area consists of poor aquifer protective capacity. The results from this study show that the whole study area is characterized by moderate to good and to some extent very good aquifer protective area. The procedures and information produced in this study may help in exploring the aquifer characteristics and groundwater quality for cost effective and sustainable agriculture.

## References


Aamer M, Sabir MF. 2014. Irrigation water quality based on hydro chemical analysis, district Rahim Yar Khan, Pakistan. Journal of Resources Development and Management, 4: 52-56.

Abbas F, Ahmad A, Safeeq M, *et al.* 2014. Changes in precipitation extremes over arid to semiarid and subhumid Punjab, Pakistan. Theoretical and Applied Climatology, 116(3-4): 671-680.

Adagunodo TA, Akinloye MK, Sunmonu LA, *et al*. 2018. Groundwater exploration in Aaba residential area of Akure, Nigeria. Frontiers in Earth Science, 6: 66. https://doi.org/10.3389/feart.2018.00066

Adeniji A, Obiora D, Omonona O, *et al.* 2013. Geoelectrical evaluation of groundwater potentials of Bwari basement area, Central Nigeria. International Journal of Physical Sciences, 8(25): 1350-1361.

Akinwumiju AS, Olrunfemi MO, Afolabi O. 2016. GIS-based integrated groundwater poten-tial assessment of Osun Drainage Basin, Southwestern Nigeria. Ife Journal of Science, 18(1): 147-168.

Alam N, Olsthoorn TO. 2014. Punjab scavenger wells for sustainable additional groundwater irrigation. Agricultural Water Management, 138(31): 55-67.

Basharat M, Tariq A. 2013. Long-term groundwater quality and saline intrusion assessment in an irrigated environment: A case study of the aquifer under the lbdc irrigation system. Irrigation and Drainage, 62(4): 510-523. DOI: 10.1002/ird.1738

Basharat M, Sultan S, Malik A. 2015. Groundwater management in Indus Plain and integrated water resources management approach. International Waterlogging and Salinity Research Institute (IWASRI): Lahore, Pakistan.

Basharat M, Tariq A-U-R. 2014. Command-scale integrated water management in response to spatial climate variability in Lower Bari Doab Canal irrigation system. Water Policy, 16(2): 374-396. https://doi.org/10.2166/wp.2013.221

Bureau of Statistics, Government of Punjab. 2014. Statistics division. Lahore. 2014-15

Charoenpong S, Suwanprasit C, Thongchumnum P. 2012. Impacts of interpolation techniques on groundwater potential modeling using GIS in Phuket Province, Thailand. Andaman Environment and Natural Disaster Research Center.

Daraz GK, Wahedullah, Bhatti AS. 2013. Groundwater investigation by using resistivity survey in Peshawar, Pakistan. Journal of Resources Development and Management, 2: 9-20.

Dor N, Syafalni S, Abustan I, *et al.* 2011. Verification of surface groundwater connec-tivity in an irrigation canal using geophysical, water balance and stable isotope approaches. Water Resource Management, 5: 2837.

El-Kadi AI. 2017. Groundwater models for resources analysis and management. CRC Press.

Elliott J, Deryng D, Müller C, *et al*. 2014. Constraints and potentials of future irrigation water availability on agricultural production under climate change. Proceedings of the National Academy of Sciences, 111(9): 3239-3244. www.pnas.org/cgi/doi/10.1073/pnas.1222474110

GOP. 2017. Agriculture statistics of Pakistan 2017-18. Ministry of National Food Security and Research Islamabad.

Hasan M, Shang Y, Akhter G, *et al*. 2018. Geophysical assessment of groundwater potential: A case study from Mian Channu Area, Pakistan. Ground Water, 56(5): 783-796. DOI: 10.1111/gwat.12617

Hasan M, Shang Y, Akhter G, *et al*. 2017. Geophysical investigation of fresh-saline water

interface: A case study from South Punjab, Pakistan. Ground Water, 55(6): 841-856. DOI: 10.1111/gwat.12527.

Imran M, Ali A, Ashfaq M, *et al*. 2018. Impact of climate smart agriculture (CSA) practices on cotton production and livelihood of farmers in Punjab, Pakistan. Sustainability. 10:2101.

Kearey P, Brooks M, Hill I. 2013. An introduction to geophysical exploration. John Wiley & Sons.

Khan AD, Iqbal N, Ashraf M, *et al*. 2016. Groundwater investigation and mapping in Upper Indus Plain. Pakistan Council of Research in Water Resources (PCRWR), Islamabad: 72.

Koefoed O. 1979. Groundwater principles, 1, Resistivity sounding measurements. Elsevier Scientific Publication co, Amsterdam-Oxford-New York.

Maillet R. 1947. The fundamental equations of electrical prospecting. Geophysics, 12(4): 529-556. DOI: 10.1190/1.1437342

Manu E, Agyekum WA, Duah A, *et al*. 2019. Application of vertical electrical sounding for groundwater exploration of cape coast municipality in the central region of Ghana. Arabian Journal of Geosciences, 12(6): 196. DOI: 10.1007/s12517-019-4374-4

Mehmood Q, Mehmood W, Awais M, *et al*. 2020. Optimizing groundwater quality exploration for irrigation water wells using geophysical technique in semi-arid irrigated area of Pakistan. Groundwater for Sustainable Development: 100397. https://doi.org/10.1016/j.gsd.2020.100397

Michael F, Reilly TE, Michael GR, *et al.* 2003. Assessing groundwater vulnerability to contamination: Providing scientifically defensible information for decision makers. US Geological Survey Circular: 1224.

Mohamaden M, El-Sayed H, Hamouda A. 2016. Combined application of electrical resistivity and GIS for subsurface mapping and groundwater exploration at El-Themed, Southeast Sinai, Egypt. The Egyptian Journal of Aquatic Research, 42(4): 417-426. DOI: 10.1016/j.ejar.2016.10.007

Mujtaba G, Ahmed Z, Ophori D. 2007. Management of groundwater resources in Punjab, Pakistan, using a groundwater flow model. Journal of Environmental Hydrology, 15: 1-14.

Nas B, Berktay A. 2010. Groundwater quality mapping in urban groundwater using GIS. Environmental Monitoring and Assessment, 160(1-4): 215-227.

Nwachukwu S, Bello R, Balogun A. 2019. Evaluation of groundwater potentials of Orogun, South-south part of Nigeria using electrical resistivity method. Applied Water Science, 9(8): 184. DOI: 10.1007/s13201-019-1072-z

Obianwu VI, Atan O, Okiwelu O. 2015. Determination of aquifer position using electric geophysical method. Applied Physics Research, 7(2): 83.

Oladapo MI, Akintorinwa OJ. 2007. Hydrogeophysical study of Ogbese south western Nigeria. Global Journal of Pure and Applied Sciences, 13(1): 55-61. DOI: 10.4314/gjpas.v13i1.16669

Punthakey J, Khan M, Ahmad RN, *et al*. 2016. Optimising canal and groundwater management to assist water user associations in maximizing crop production and managing salinisation in Australia and Pakistan.

Shakir AS, Mughai H, Khan NM, *et al*. 2016. Impact of canal water shortages on groundwater in the Lower Bari Doab Canal System in Pakistan. Pakistan Journal Engineering & Application Science, 9: 87-97.

Shakoor A. 2015. Hydrogeologic assessment of spatio-temporal variation in groundwater quality and its impact on agricultural productivity, University of Agriculture, Faisalabad.

Sikandar P, Christen E, Stein TM. 2017. Vertical electrical sounding (ves) for salinity assessment of water-bearing formations. Irrigation and Drainage, 66(2): 252-262. DOI: 10.1002/ird.2094

Singh KP. 2005. Nonlinear estimation of aquifer parameters from surficial resistivity measurements. Hydrology and Earth System Sciences Discussions, 2(3): 917-938. DOI: 10.5194/hessd-2-917-2005.

Terry N, Day-Lewis F, Robinson JL, *et al.* 2017. Scenario evaluator for electrical resistivity survey pre-modeling tool. Groundwater, 55(6): 885-890. https://doi.org/10.1111/gwat.12522

WAPDA. 1980. Hydrological data of Bari Doab,

basic data release. Directorate General of Hydrogeology, Lahore.

WAPDA. 1981. Atlas-Soil salinity survey of irrigated areas of Indus basin 41 million acres. Survey and Research Organization, Planning Division, Lahore, WAPDA.

Watto MA, Mugera AW. 2016. Groundwater depletion in the Indus plains of Pakistan: Imperatives, repercussions and management issues. International Journal of River Basin Management, 14(4): 447-458. https://doi.org/10.1080/15715124.2016.1204154.

Yeboah-Forson A, Whitman D. 2013. Electrical resistivity characterization of anisotropy in the Biscayne aquifer. Ground Water, 52: 728-736. DOI: 10.1111/gwat.12107